Journal of Hazardous Materials 198 (2011) 31–39

Contents lists available at SciVerse ScienceDirect

Journal of Hazardous Materials

journal homepage: www.elsevier.com/locate/jhazmat

Metal-induced phosphate extracellular nanoparticulate formation in *Ochrobactrum tritici* 5bvl1

Romeu Francisco[a], Pedro de Abreu[a], Bradley A. Plantz[d], Vicki L. Schlegel[c], Rui A. Carvalho[b], Paula Vasconcelos Morais[a,b,*]

[a] *IMAR-CMA, 3004-517 Coimbra, Portugal*
[b] *Department of Life Sciences, FCTUC, University of Coimbra, 3001-401 Coimbra, Portugal*
[c] *Food Science and Technology, University of Nebraska-Lincoln, United States*
[d] *Department of Biology, University of Nebraska-Kearney, United States*

ARTICLE INFO

Article history:
Received 31 May 2011
Received in revised form 9 September 2011
Accepted 2 October 2011
Available online 7 October 2011

Keywords:
Chromium
Toxicity
Resistant bacteria
Phosphate complexes

ABSTRACT

Hexavalent chromium (Cr(VI)) is a toxic environmental contaminant which detoxification consists in reduction to Cr(III). In this work, the Cr(VI)-resistant and reducing *Ochrobactrum tritici* 5bvl1 produced phosphate nanoparticles upon exposure to Cr(VI) and Fe(III), effectively removing chromium from solution. Under Cr(VI) stress, higher siderophore production by strain 5bvl1 was observed. Cr(VI) toxicity was decreased in presence of Fe(III), increasing the growth and Cr(VI)-reduction rates in cell cultures, lowering the amount of morphologically compromised cells and promoting chromium immobilization as insoluble extracellular phosphate complexes. The formation of phosphate nanoparticles increased with Cr(VI) and Fe(III) concentrations and was also stimulated by Ni(II). Under these experimental conditions, nanoparticle formation occurred together with enhanced inorganic phosphate consumption by cells and increased polyphosphate kinase (PPK) activity. NMR analysis of the particles showed the presence of both polyphosphate and phosphonate together with orthophosphate, and FT-IR supported these results, also showing evidences of Cr(III) coordination. This work demonstrated that *O. tritici* 5bvl1 possesses protection mechanisms against chromium toxicity other than the presence of the Cr(VI) pump and SOD related enzymes previously described. Future assessment of the molecular regulation of production of these nanoparticles will open new perspectives for remediation of metal contaminated environments.

1. Introduction

Hexavalent chromium (Cr(VI)) is a carcinogenic environmental contaminant [1]. Remediation of contaminated soils and waters is achieved by reducing Cr(VI) to the less toxic and less soluble trivalent chromium (Cr(III)) using microorganisms [2].

Several Cr(VI)-resistant bacteria species have been isolated in recent years. Cr(VI)-resistance is a consequence of the summed effects of various strategies, which include Cr(VI) reduction to Cr(III) aerobically or anaerobically [3–6], repair of damaged DNA, proteins and lipids, free-radical scavenging enzymes and the efflux of Cr(VI) from the cytoplasm [7], or downregulation of the sulfate transport system, responsible for chromate uptake [8]. Among the most resistant microorganisms are the strains *Brevibacterium* sp. CrT-13 [9], *Ochrobactrum intermedium* SDCr-5 [10] and *Ochrobactrum tritici* 5bvl1 [11].

The efflux of chromate is performed by the membrane-potential dependent ChrA membrane transporter [12], a protein coded by the *chrA* gene, present in *Pseudomonas aeruginosa* (plasmid pUM505) [13], in *Cupriavidus metallidurans* (plasmid pMOL28) [14] and in *O. tritici* 5bvl1 (transposon Tn*OtChr*) [15]. In this last microorganism, transposon Tn*OtChr* contains the operon *chrBACF*, which also codes a regulatory protein, ChrB, responsible for the induction of the *chrA* gene and a superoxide dismutase (SOD), ChrC [15].

Metal sequestration and precipitation occurs in several bacteria, but the contribution of this phenomenon to cell survival under metal stress is not fully understood. Microbiological metal precipitation in extracellular phosphate complexes was previously reported as important in uranium or chromium bioremediation strategy [2,16]. Recently, after Cr(VI) reduction by bacterial consortia, Cr(III) was found coordinated octahedrically to phosphate in the biofilm [17]. In contrast, phosphate solubilization by plant growth-promoting bacteria under metal stress leads to a higher heavy metal bioavailability which results in uptake by plants [18]. In recent reports, polyphosphates and phosphonates were found in abundance in marine sediments, and suggested to originate from benthic microorganisms, in response to redox potential changes [19]. Until

* Corresponding author at: Department of Life Sciences, FCTUC, University of Coimbra, 3001-401 Coimbra, Portugal. Tel.: +351 239 824024; fax: +351 239 855789.
E-mail address: pvmorais@ci.uc.pt (P.V. Morais).

0304-3894/$ – see front matter © 2011 Elsevier B.V. All rights reserved.
doi:10.1016/j.jhazmat.2011.10.005

today however, there is a lack of evidences linking polyphosphates to the metal-phosphate extracellular aggregates produced by bacteria.

O. tritici strain 5bvl1 was used in this work as a model. This strain was isolated from a Cr(VI)-contaminated wastewater treatment plant [20], and is one of the most Cr(VI)-resistant microorganisms known [11], as opposed to *O. tritici* SCII24^T [21]. Strain 5bvl1 possesses capacity to reduce Cr(VI) and was shown in the current work to form insoluble extracellular nanoparticles in presence of this metal, provided Fe(III) was also available. Consequently, the goals of this work include the study of the chemical structure of the nanoparticles, and of its metal dependence. To achieve these goals, siderophore production was followed in presence of Cr(VI), nanoparticles were characterized by SEM-EDS, FT-IR and ^{31}P NMR, and total phosphate present in nanoparticles and growth medium was quantified and correlated to the concentrations of metals present in solution. Polyphosphate kinase (PPK) activity of cell extracts was tested on cells exposed to metals. Physiological assays were also performed in order to determine if the presence of iron and nanoparticle formation improved the Cr(VI) resistance and reduction abilities of the model strain.

2. Experimental

2.1. Bacteria strains

O. tritici strain 5bvl1 was isolated from activated sludge in a chromium-contaminated area [20]. The type strain *O. tritici* SCII24^T was obtained from LMG Culture Collection (Gent, Belgium) and is Cr(VI)-sensitive. The strains were maintained at −80 °C in Nutrient Broth (Difco) containing 15% (w/v) glycerol.

2.2. Growth conditions and Cr(VI) quantification in resistance assays

The strain was cultured in buffered mineral medium (MMH) [12] using double-distilled water (ddH_2O) and incubated at 30 °C. Growth was determined by optical density (O.D.) at 600 nm. The glass apparatus was previously washed with concentrated HNO_3 to remove trace amounts of iron and washed thoroughly with ddH_2O. The assays performed with iron contained 100 μM $FeCl_3$ while iron-deprived assays contained less than 2 μM Fe. Chromium was used either as sodium dichromate ($Na_2Cr_2O_7$) or sodium chromate (Na_2CrO_4), ranging from 0 to 4 mM. Cr(VI) concentration in culture was followed using the diphenylcarbazide method [22]. Total chromium present in cell pellets was quantified using the same method after re-oxidation of Cr(III) with $KMnO_4$ [22]. All assays were performed in triplicate and are expressed as averages, with standard deviation.

2.3. Siderophores

Strain 5bvl1 was tested positive for siderophore production in Chrome Azurol S (CAS) agar medium incubated at 30 °C. The strain was then tested for the presence of soluble siderophores in MMH and for the presence of membrane-bound siderophores. The assays consisted of inoculated MMH with 2 mM Cr(VI) as chromate or dichromate, and with or without $FeCl_3$. Soluble siderophores were tested with CAS, Arnow's assay, for catechol-type siderophores, and Atkin's assays, for hydroxamate-type siderophores, as described by Clark [23]. Membrane-bound ochrobactin-like siderophores were extracted with ethanol from cells recovered from the culture (2 ml) [24]. The extract was concentrated by evaporation, applied on CAS agar medium, and plates were incubated at room temperature for 48 h before digitalization, densitometry analysis and normalization.

2.4. Scanning electron microscopy with X-ray microanalysis (SEM-EDS)

Strain 5bvl1 was grown for 72 h in MMH with 2 mM Cr(VI) as chromate or dichromate, and either under iron deficiency, or with 100 μM Fe(III). Cell samples were prepared and solidified in blocks of Spurr resin (TAAB) as previously described [12]. Samples were thin sectioned, applied to a copper grid and analysed by a Jeol JSM 6301F scanning electron microscope coupled with EDS (Oxford INCA 350).

2.5. Nanoparticle metal-dependent formation

Cells suspensions were obtained from cultures that reached stationary phase after 72 h, at 30 °C, in MMH under iron deficiency and supplemented with 0.25 mM Na_2CrO_4. Cells were concentrated, washed and resuspended in MMH medium. Nanoparticle metal-dependence was tested on cell suspensions in 20 ml MMH medium with an initial O.D. of 2.0.

2.5.1. Effect of iron

To evaluate the iron nanoparticle formation dependence, assays were performed with cell suspensions containing 2 mM Na_2CrO_4 and $FeCl_3$ concentrations of 0, 50, 100, 150, 200, 250 and 300 μM. Assays were incubated at 30 °C during 96 h and sampled (2 ml) at set time intervals. Cr(VI) was quantified from samples as described in Section 2.2. Reduction rates were compared by one-way ANOVA analysis followed by Dunett's multiple comparison post-test. Cells were resuspended in 1 ml ddH_2O and subjected to sucrose gradient centrifugation (4 °C, 3220 × *g*, 30 min), with the following 2 ml sucrose phases, from bottom to top: 70%, 45%, 30%. The pellet formed was further purified after resuspension in 500 μl ddH_2O and centrifugation against a 1:1 85% sucrose phase (16,100 × *g*, 15 min). The 45% sucrose phase contained most cells, while the 85% sucrose phase contained a pellet of purified metal-rich aggregates. Total intracellular phosphate and phosphate from aggregates were quantified using an ascorbic acid method [25] after 2 washes with ddH_2O (3220 × *g*, 15 min), resuspension in 1 ml ddH_2O and HCl digestion at 120 °C, during 45 min. All assays were performed in triplicate and averages of three values were plotted with standard deviations. Graphs and statistical analysis were performed using GraphPad Prism v5.0 for windows, GraphPad software, San Diego, California, USA, www.graphpad.com.

2.5.2. Effect of chromium

To evaluate the chromium nanoparticle formation dependence, assays were performed with cell suspensions containing 300 μM $FeCl_3$ and Na_2CrO_4 concentrations ranging from 0 to 5 mM. Free phosphate ions present in the suspension and phosphate from the nanoparticles were quantified as described in Section 2.5.1. Cr(VI) was quantified for the *O. tritici* strain 5bvl1 assays. The different responses were compared by one-way ANOVA analysis followed by Turkey's multiple comparison and linear trend post-tests.

2.5.3. Effect of other metals and paraquat

All samples were processed and analysed as in Section 2.5.1. Assays containing an initial concentration of 1 mM of: paraquat, $NaAsO_2$ (As(III)), $HAsNa_2O_4$ (As(V)) or $NiCl_2$ (Ni(II)) were compared with 1 mM Cr(VI).

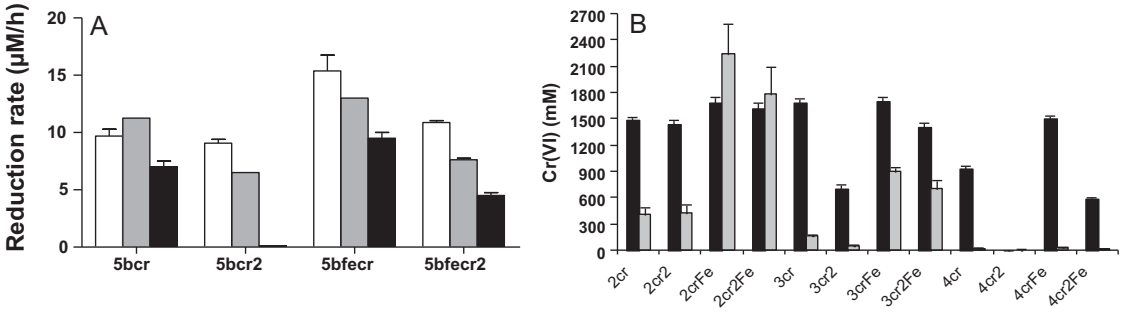

Fig. 1. A. Cr(VI) reduction rate of *O. tritici* 5bvl1 cultures with 100 μM $FeCl_3$ and increasing concentrations of chromate or dichromate. 5bcr: chromate; 5bfecr: chromate and iron; 5bcr2: dichromate; 5bfecr2: dichromate and iron. Symbols: (□) 2 mM Cr(VI); (▒) 3 mM Cr(VI); (■) 4 mM Cr(VI). B. Total reduced Cr(VI) and insoluble chromium in *O. tritici* 5bvl1 cultures with increasing Cr(VI) concentrations and 100 μM $FeCl_3$, after 190 h. Assays: NCr(2)(Fe), where N = Cr(VI) concentration (2–4 mM), Cr = chromate while Cr2 = dichromate, and Fe = assays with 100 μM $FeCl_3$. Symbols: (■) total reduced chromium; (▒) total insoluble chromium.

2.6. PPK activity

O. tritici 5bvl1 cell samples were obtained from MMH cultures, either metal-free (control) or supplemented with 2 mM Cr(VI) and 100 μM $FeCl_3$. The presence of polyphosphate granules in samples was checked with a Neisser stain [26], while cell crude extracts were tested for PPK activity. Cell extracts were obtained by sonication from cells suspensions in Tris–HCl buffer pH 7.0, followed by centrifugation (4 °C, 3220 × *g*) to remove cell debris, and were treated with a protease inhibitor cocktail tablet (Roche). PPK activity was measured as described by Mullan et al. [27], through the metachromatic reaction of toluidine blue with polyphosphate. Assays were performed in triplicate and are expressed as averages, with standard deviation.

2.7. Spectroscopic analysis

2.7.1. ^{31}P NMR

Purification of extracellular aggregates from strain 5bvl1 cultures in MMH with 2 mM Cr(VI) and 100 μM $FeCl_3$ was performed as in Section 2.5.1. Samples were washed and subsequently resuspended in 350 μl ^2H_2O (99.97%) for ^{31}P NMR analysis. This volume was added to a 5 mm NMR tube, and a solution of H_3PO_4 85% in a capillary tube, which was inserted into the 5 mm NMR tube, was used as a chemical shift standard (0.0 ppm). Due to the overall low solubility of the samples, extensive signal averaging (number of scans ≥1,000,000) was required for each NMR spectrum. Typical acquisition parameters included an acquisition time of 50 milliseconds (ms), corresponding to 2048 points covering a spectral width of 24.5 kHz. Before Fourier transformation a 50 Hz Lorentzian apodization function was applied to the free induction decay (FID) to improve signal to noise ratio.

2.7.2. FT-IR

To perform FT-IR analysis, extracellular aggregates were purified as in Section 2.5.1. One sample was washed with ddH_2O and lyophilized and another was washed with acetone to wash away contaminant cells and phospholipids, and finally dried at 70 °C. Standards were obtained by lyophilizing solutions of pure Graham's salt, or mixtures containing $CaCl_2$, $FeCl_3$ or $CrCl_3$. FT-IR analysis and spectra acquisition and manipulation were performed on a Bruker Equinox 55 FT-MIR in ATR mode, using the Bruker Opus 4.0 software at the University of Nebraska-Lincoln, USA. Spectra were obtained over the mid-IR region (4000–750 cm^{-1}) at a resolution of 4 cm^{-1}. To increase signal to noise, each spectrum was collected as an average of 64 scans, apodized with the Blackman–Harris 3-Term function and then Fourier-transformed. The spectra were baselined corrected and reported as the zero order data.

3. Results

3.1. Effect of iron on bacterial growth in presence of Cr(VI)

Different toxicities are attributed to the two anionic forms of Cr(VI), dichromate and chromate, with the first one showing the highest toxicity [12]. In iron-deficient MMH, strain 5bvl1 was markedly more sensitive to dichromate and growth was almost totally inhibited with 2 mM $Na_2Cr_2O_7$ (4 mM Cr(VI)), comparatively to 4 mM Na_2CrO_4. The addition of 100 μM $FeCl_3$ to the growth medium resulted in higher optical densities (O.D.) in stationary phase for all assays without clearly increasing the growth rate (variation <10%). However, in presence of 2 mM $Na_2Cr_2O_7$, growth performed better than under iron deficiency, with a rate increase of 84.4%. The media containing Fe(III) showed cell aggregation, particularly visible with 2 mM Cr(VI). In those experimental conditions, a green sediment formed, which was not detected in the absence of iron.

3.2. Cr(VI) reduction

Reduction rates occurred at maximal speed after the end of the exponential phase of growth and started to decrease after the reduction of 1–1.5 mM Cr(VI).

The reduction rates of cells grown in presence of Cr(VI), both as chromate or dichromate, were always higher when iron was present (Fig. 1A). The highest reduction rate obtained in cultures was of 15.4 ± 1.4 μM/h in 2 mM chromate and 100 μM $FeCl_3$. Iron caused a higher rate increase in cultures with chromate, except at 4 mM Cr(VI), where it allowed cultures with dichromate to increase rates from zero to 4.5 ± 0.2 μM/h.

The maximum total amount of Cr(VI) reduced by strain 5bvl1 in culture varied between 1400 and 1700 μM after 190 h (Fig. 1B). Higher Cr(VI) concentrations resulted in lower values but the presence of iron improved those results. In the assays performed under iron shortage, total reduced Cr(VI) was visibly inhibited at 4 mM chromate, As for dichromate assays, under iron shortage, inhibition was strong at 3 mM Cr(VI) and total at 4 mM Cr(VI). In presence of iron, inhibition was only detected in the dichromate assays at the highest Cr(VI) concentration tested (4 mM).

The amount of insoluble chromium in cultures, under iron shortage, was residual (<10%) at all tested Cr(VI) concentrations. In cultures with Fe(III), at 2 mM Cr(VI), chromium immobilization occurred simultaneously to Cr(VI) disappearance, and Cr that was reduced matched Cr found in an insoluble form, at any given time of incubation. Higher concentrations of Cr(VI) in cultures with Fe(III) inhibited the immobilization: in 50–60% at 3 mM Cr(VI), and almost 100% at 4 mM Cr(VI) (Fig. 1B).

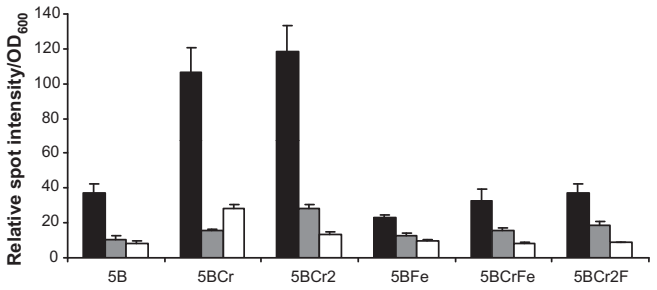

Fig. 2. Membrane-bound siderophore production. Spot intensities generated in CAS agar medium per culture O.D. at different growth phases. Symbols: (■) middle of exponential phase; (▩) end of exponential phase; (□) stationary phase.

3.3. Presence of siderophores

No soluble siderophores were found in the medium in any tested conditions.

In contrast, the membrane extracts of all cells cultured without Fe(III) generated positive reaction on CAS medium. The most intense reactions were generated by samples from middle exponential growth phase (Fig. 2). The highest siderophore production was from culture samples containing Cr(VI) and no Fe(III). The absence of Cr(VI) in medium with Fe(III) led to the lowest production of siderophores. However, samples with Fe(III) and Cr(VI) showed a siderophore production comparable to the assay performed in absence of both metals.

3.4. SEM-EDS

In all samples, most cells possessed 1–2 dense intracellular granules containing phosphorus, oxygen and calcium. Under iron deficiency, cell samples were devoid of extracellular structures, both in presence or absence of Cr(VI), and more morphologically compromised cells were observed (Fig. 3A). Rare extracellular aggregates were found in absence of Cr(VI) and presence of Fe(III), containing O, P, Fe, Mg and Ca (Fig. 3C). In contrast, cells grown in presence of Cr(VI) and supplemented with 100 μM $FeCl_3$ produced a great amount of dark green amorphous (confirmed by X-ray diffraction) and dense extracellular aggregates (Fig. 3B and D). These aggregates were composed of P, O, Ca, Fe, Cr and low amounts of Mg and Na (Fig. 3E and F). Under these experimental conditions, cytosol and membranes of morphologically uncompromised cells were free of detectable quantities of iron and chromium, while morphologically compromised cells possessed low quantities of chromium in intracellular denser areas enriched in P and Ca.

3.5. Metal-dependent formation of phosphate-containing aggregates

As EDS spectra provided evidences of the presence of phosphate, quantification of inorganic phosphate (Pi) present in the purified dense extracellular particles formed in presence of Fe(III) and Cr(VI) was made. The phosphate quantity present in the extracellular aggregates was found to increase with Fe(III) and Cr(VI) concentrations, both for strain 5bvl1 and *O. tritici* type strain (Fig. 4).

When testing the effect of Fe(III) on the cell suspensions capacity to produce phosphate-rich extracellular aggregates, in presence of 2 mM Na_2CrO_4, the highest Pi amount present in extracellular aggregates was found at the highest Fe(III) concentration tested (300 μM), Under those experimental conditions, the Pi quantity obtained from 2 ml of medium after 96 h of incubation was of 0.42 ± 0.11 μmol for strain 5bvl1 and of only 0.28 ± 0.06 μmol for the *O. tritici* type strain. In contrast, under iron deficiency, the Pi quantity was of 0.07 ± 0.02 μmol and 0.03 ± 0.01 μmol for strain 5bvl1 and *O. tritici* type strain, respectively (Fig. 4A). Extracellular Pi in both strains was approximately the same up to 200 μM $FeCl_3$ (0.23 ± 0.12 μmol for strain 5bvl1 against 0.18 ± 0.01 μmol for the type strain after 96 h of incubation), but became higher for strain 5bvl1 at higher Fe(III) concentration (0.29 ± 0.07 μmol for strain 5bvl1 against 0.14 ± 0.01 μmol for the type strain at 250 μM Fe(III)).

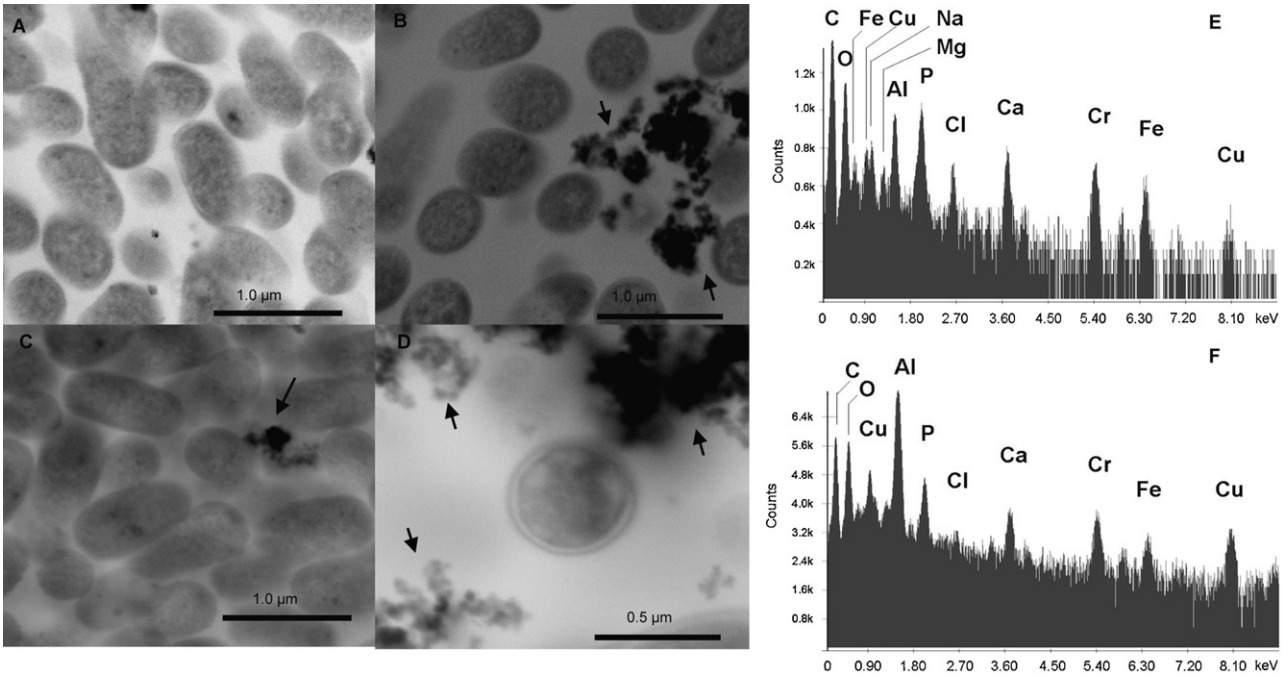

Fig. 3. Extracellular aggregates formed in *O. tritici* 5bvl1 cultures exposed to iron and Cr(VI). Arrows show extracellular aggregates containing Cr and Fe. A – cultures with 2 mM Cr(VI) (chromate); B – cultures with 100 μM $FeCl_3$ and 2 mM Cr(VI) (chromate); C – cultures with 100 μM $FeCl_3$; D – cultures with 100 μM $FeCl_3$ and 2 mM Cr(VI) (dichromate). E and F – EDS spectra of extracellular aggregates respectively found in (B) or (D).

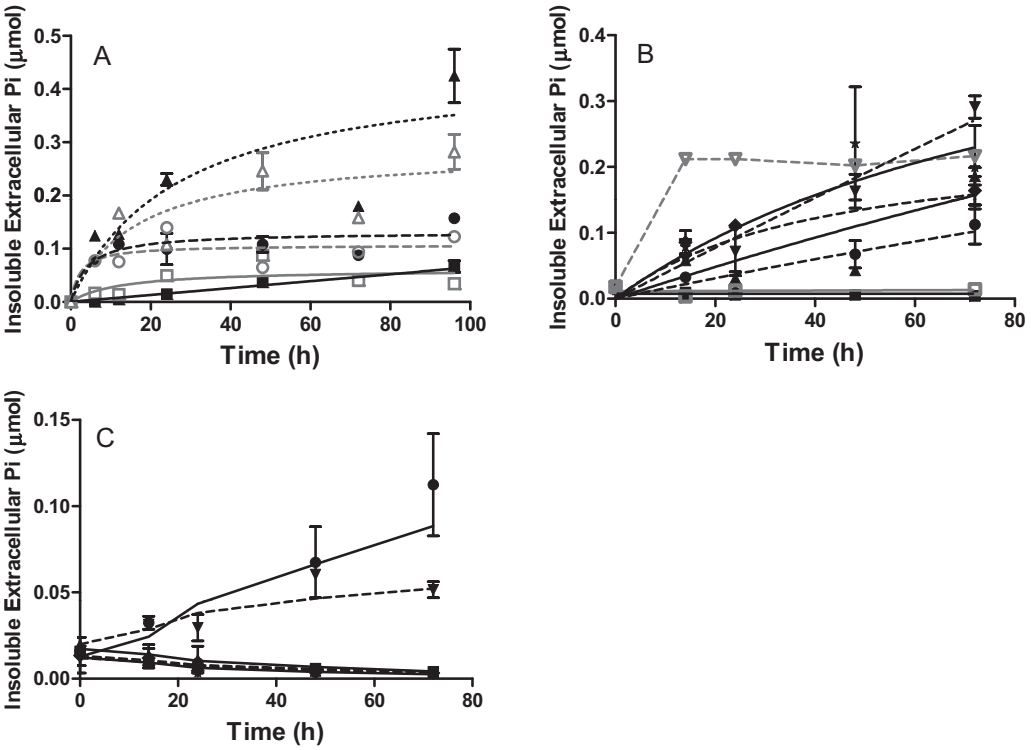

Fig. 4. Extracellular aggregates dependence of: (A) $FeCl_3$, in presence of 2 mM Cr(VI); (B) Cr(VI), in presence of 300 μM $FeCl_3$; (C) Cr(VI) substitutes, in presence of 300 μM $FeCl_3$. Symbols: full – *O. tritici* 5bvl1; open – *O. tritici* type strain; fl – full lines; dl – dashed lines; dt – dotted lines. (A): ■□(fl) – 0 μM $FeCl_3$; ●○(dl) – 150 μM $FeCl_3$; ▲△(dt) – 300 μM $FeCl_3$. (B): ■□(fl) – no Cr(VI); ●(dl) – 1 mM Cr(VI); ▲(fl) – 2 mM Cr(VI); ♦(dl) – 3 mM Cr(VI); ⋆(fl) – 4 mM Cr(VI); ▼▽(dl) – 5 mM Cr(VI). (C): ■(dl) – no Cr(VI); ●(fl) – 1 mM Cr(VI); ▲(fl) – 1 mM paraquat; ♦(dl) – 1 mM $NaAsO_2$; ⋆(fl) – 1 mM K_3AsO_4; ▼(dl) – 1 mM $NiCl_2$. Curves were fitted to the data either by nonlinear regression, using an enzyme kinetics model (A and B) or by applying a second order smoothing polynomial curve.

When testing the effect of Cr(VI) in the presence of 300 μM Fe(III), the phosphate content of strain 5bvl1 extracellular aggregates increased with the Cr(VI) concentration (Fig. 4B). The highest Pi amount after 72 h was of 0.29 ± 0.02 μmol for strain 5bvl1 and 0.21 ± 0.01 μmol for the type strain in presence of 5 mM Cr(VI), while no Pi was detected in absence of Cr(VI).

Of the tested Cr(VI) metal substitutes (As(III), As (V), Ni(II), and paraquat), only Ni(II) was able to cause the production of insoluble extracellular aggregates containing phosphate, but in a lower quantity than Cr(VI) (Fig. 4C).

3.6. Intracellular phosphate

In presence of 2 mM Cr(VI), the total intracellular phosphate increased when $FeCl_3$ was added to the medium. Intracellular phosphate of 2 ml samples started at 0.014 ± 0.001 μmol, then rapidly increased before stabilizing after 24 h. The iron concentrations that caused the highest intracellular increases were 250 μM $FeCl_3$ for strain 5bvl1 (0.065 ± 0.014 μmol after 96 h) and 250–300 μM $FeCl_3$ for the type strain (0.064 ± 0.002 μmol after 96 h and 0.088 ± 0.005 μmol after 48 h, respectively), with increases superior to 4 fold of the initial value. In the absence of iron, the maximum values of total intracellular phosphate were for strain 5bvl1 0.052 ± 0.011 μmol and for *O. tritici* type strain 0.049 ± 0.004 μmol, both obtained after 24 h incubation.

3.7. Soluble extracellular phosphate

The extracellular phosphate concentration of the growth medium used decreased when cells were exposed to Cr(VI) and 300 μM Fe(III) (Fig. 5A). At Cr(VI) concentrations of 1–3 mM, the Pi decrease reached approximately 0.13 mM (0.26 μmol Pi in 2 ml MMH). At higher Cr(VI) concentrations, the final Pi concentration of the medium was higher.

In presence of Cr(VI) substitutes, phosphate depletion was less effective (Fig. 5B). As(V) failed, and paraquat caused a depletion inferior to 0.05 mM Pi during the whole incubation period. As(III) caused after 48 h a phosphate disappearance comparable to paraquat. Ni(II) caused an effect similar to Cr(VI), reaching 0.10 mM of Pi depletion.

3.8. Cr(VI) reduction rates by cell suspensions

With 2 mM Cr(VI) and increasing iron concentrations, no increase to the Cr(VI) reduction rates of cell suspensions were observed, both for strain 5bvl1 and the type strain (Fig. 6A) as most experimental conditions did not show statistically significant differences with the control (0 μM Fe(III)). On the other hand, in presence of 300 μM Fe(III), the reduction rates of strain 5bvl1 cell suspensions increased linearly with increasing Cr(VI) concentrations, showing no inhibition, unlike cell cultures (Fig. 6B). At 5 mM Cr(VI), the reduction rate obtained was of 17.7 μM/h.

3.9. PPK activity

The presence of abundant polyphosphate granules produced by 5bvl1 and *O. tritici* type strain in presence of Fe(III) and Cr(VI) was confirmed with a Neisser stain, in contrast to cells grown without those metals.

The PPK activity assay revealed that polyphosphate production of extracts of cells grown in presence of Cr(VI) and Fe(III) was enhanced, reaching 10.05 ± 3.56 mg/L of standard polyphosphate equivalent (Fig. 7), while the polyphosphate produced in absence of these metals was very low (0.92 ± 6.32 mg/L).

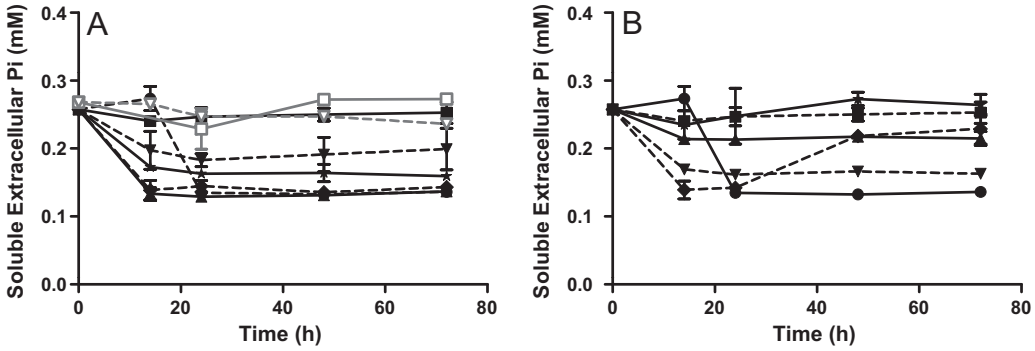

Fig. 5. Soluble phosphate concentration in MMH with 300 μM $FeCl_3$. (A) Dependence of Cr(VI); (B) dependence of Cr(VI) substitutes. Symbols: full – *O. tritici* 5bvl1; open – *O. tritici* type strain; fl – full lines; dl – dashed lines. (A): ■□(fl) – no Cr(VI); ●(dl) – 1 mM Cr(VI); ▲(fl) – 2 mM Cr(VI); ♦(dl) – 3 mM Cr(VI); ⋆(fl) – 4 mM Cr(VI); ▼▽(dl) – 5 mM Cr(VI). (B): ■(dl) – no Cr(VI); ●(fl) – 1 mM Cr(VI); ▲(fl) – 1 mM paraquat; ♦(dl) – 1 mM $NaAsO_2$; ⋆(fl) – 1 mM K_3AsO_4; ▼(dl) – 1 mM $NiCl_2$.

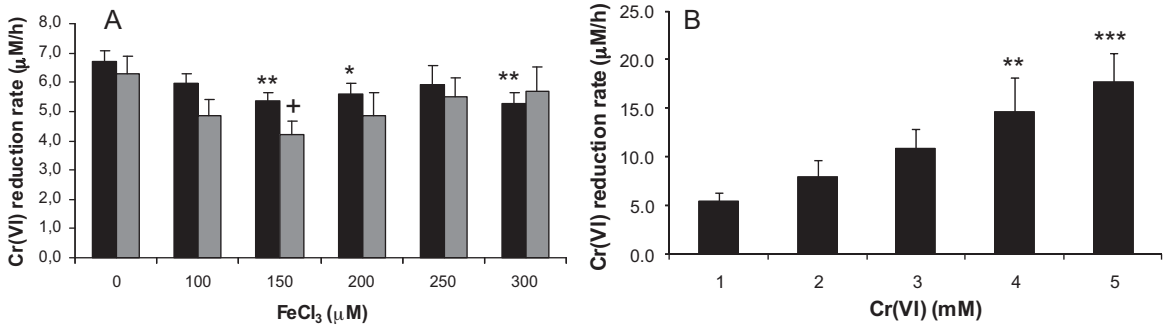

Fig. 6. Cr(VI) reduction rates of cell suspensions. A – in presence of 2 mM Cr(VI) and increasing $FeCl_3$ concentrations; Symbols: (■) *O. tritici* 5bvl1; (▩) *O. tritici* type strain. Means significantly different from control 0 μM $FeCl_3$ ($P < 0.05$) are signalled; B – *O. tritici* 5bvl1 cell suspensions in presence of 300 μM $FeCl_3$ and increasing Cr(VI) concentrations. Mean values are significantly different ($P < 0.05$; $F = 12.35$) and the linear trend is significant ($P < 0.0001$; slope 3.108, $R^2 = 0.8277$).

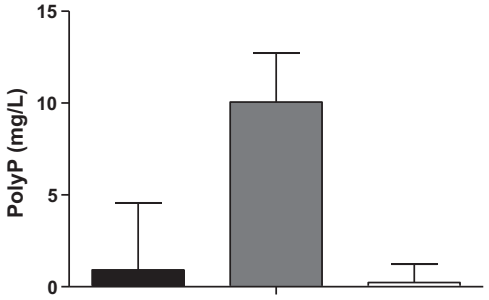

Fig. 7. PPK assay. Polyphosphate formation after 15 min, using cell extracts. Symbols: (■) cells grown in absence of Cr(VI) and Fe(III); (▩) cells grown in 2 mM Cr(VI) and 100 μM $FeCl_3$; (□) reaction buffer.

3.10. Spectroscopic analysis

^{31}P NMR analysis of the green extracellular aggregates resulted in a spectrum with phosphorus peaks at 17 ppm, −4 ppm, −14 ppm, and −24 ppm (Fig. 8) corresponding respectively to phosphonates, orthophosphate, pyrophosphate or end-chain phosphates, and polyphosphate middle-chain phosphates [19,28]. The sharpness of the signals indicates that those soluble compounds were most probably not complexed to metal ions, in particular the middle-chain phosphates [28]. Any extensive addition of DCl to promote further dissolution of the aggregates resulted in hydrolysis and concomitant increase of the resonance at −4 ppm, due to orthophosphate.

The FT-IR spectra of purified extracellular aggregates washed with water or with acetone differed remarkably (Fig. 9). The water-washed samples presented only 2 peaks in the analysed range. The first, at approximately 1640 cm^{-1}, also present in the dark green Cr(III)-PolyP control and in the acetone-washed sample, is, according to the literature, caused by the presence of Cr(III) hydroxides (Cr–O–H bond vibration), and is absent if chromium is in the hexavalent oxidation state [29]. The second was a broad signal at 1040 cm^{-1}, similar to what was previously reported in soil sediments rich in phosphates [30]. The acetone-washed sample possessed more peaks. The most intense were close to those of the controls, between 1200 and 800 cm^{-1}. Weaker signals were detected between 1500 and 1300 cm^{-1}, outside the signal range of the polyphosphate standards, and between 1300 and 1200 cm^{-1}, in the range of one of the standard peaks. The following weak signals were attributed to the residual presence of acetone and water:

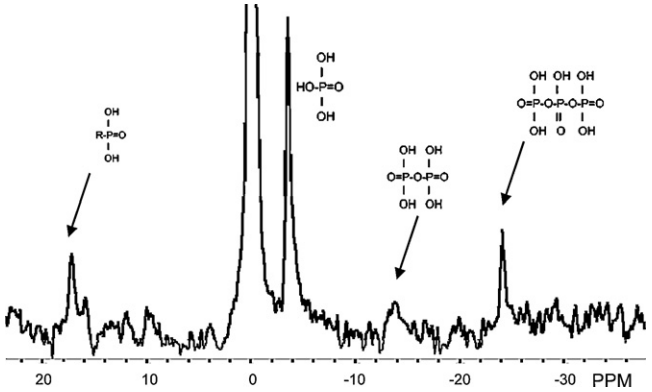

Fig. 8. ^{31}P NMR of soluble phosphate compounds after acid treatment of extracellular aggregates. Peak attribution (left to right): phosphonate, orthophosphate reference, orthophosphate, pyrophosphate or end-chain phosphate, and middle-chain phosphates.

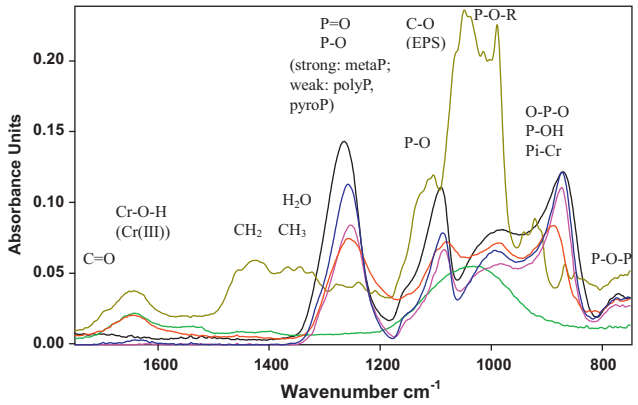

Fig. 9. FT-IR spectrum of extracellular aggregates. Symbols: black: polyphosphate standard (PPS); blue: PPS + $CaCl_2$; pink: PPS + $FeCl_3$; red: PPS + $CrCl_3$; green: sample; and brown: sample washed with acetone. (For interpretation of the references to color in this figure legend, the reader is referred to the web version of the article.)

at ~1700 cm^{-1} (C=O stretching or free water bending vibrations), between 1500 and 1300 cm^{-1} (CH_3 or hydration water bending vibrations), and at 1215–1230 cm^{-1} (C–C stretching vibration) [31]. The intense signal at approximately 1080 cm^{-1} is typical of phosphorylated compounds or exopolysaccharide (EPS) C–O vibrations [32]. All other peaks are related to phosphate compounds. At 1300–1250 cm^{-1}, the sample presented weak peaks while the polyphosphate standards showed a strong one (1260–1285 cm^{-1}). This is a region attributed to the P=O stretching bond vibration [33,34] of pyrophosphate and polyphosphates, especially intense for metaphosphates such as the 6(PO_3) standard that was used [34–36]. Because inorganic phosphate does not produce signals in that region [37,38], the weak signals obtained in the sample indicate the presence of pyrophosphate or of linear polyphosphate molecules, which yield low peak intensities due to high molecular stability and therefore lower P–O bond length variations [37]. The strong peak at 1100–1150 cm^{-1}, which in the sample appears to have been shifted to a higher frequency, is generally attributed to P–O asymmetric stretching mode of free phosphate, polyphosphate or metaphosphate [36]. The most intense peaks at 980–1080 cm^{-1} are characteristic of P–O–R bond vibrations, such as P–O–C symmetric stretching that occur in phospholipids or DNA [33]. However, none of those molecules are present in the sample, because of the acetone wash, and of the absence of DNA bases characteristic peaks [39]. The sharp signal at 980 cm^{-1} is close to the phosphate signals of ATP in the 950–930 cm^{-1} region [40], and of signals that occur in complexes of chromium with linear polyphosphate, metaphosphate or pyrophosphate [37]. The pair of peaks at 850–950 cm^{-1} occurs in phosphate–Cr(III) complexes and $H_2PO_4^-$ (P–O–H asymmetric and symmetric stretching vibrations), being absent from polyphosphate–Cr(III) complexes [37,38]. The weak signal between 805 and 740 cm^{-1}, also present in the controls used, is usually attributed to metaphosphates P–O–P rings [36] but also occurs in linear polyphosphate–Cr(III) complexes [37].

4. Discussion

Metal ion quelation by anions such as sulfide or phosphate has been previously described in bioremediation processes, and results in surface deposition or intracellular accumulation, effectively decreasing metal ion bioavailability in the environment [2,41,42]. As an example, precipitation and biosorption of uranium or chromium were shown to occur in extracellular phosphate complexes [2,16,17]. On the other hand, polyphosphate production capacity was found to be determinant for intracellular mercury accumulation in certain microorganisms [43]. In *O. tritici* strain 5bvl1, both processes are present and part of the Cr(VI) defense strategy, causing the extracellular deposition of metals into phosphate particles, regulated by iron and associated to the polyphosphate-production capacity.

The siderophores of *O. tritici* 5bvl1, as for *Ochrobactrum* sp. SP18 [24], were associated to membranes and in strain 5bvl1 increased under Cr(VI) stress. This was also reported on *Shewanella oneidensis* MR-1, where Cr(VI) caused the upregulation of iron transporters, siderophores, and storage proteins [44,45]. Moreover, the presence of Fe(III) in cultures with Cr(VI) did not inhibit siderophore production that should have occurred. Siderophore increased production under Cr(VI) stress may decrease toxicity by providing more iron as a cofactor of redox proteins such as SOD or enzymes with chromate-reductase activity [46]. Given that nanoparticles, which included Fe, depended on the presence of Fe(III), siderophore production was likely needed to gain the Fe necessary to the formation of these structures.

The importance of iron in Cr(VI) resistance strategy was confirmed. In cell cultures, Fe(III) increased the growth rate of strain 5bvl1, allowed growth at otherwise toxic Cr(VI) concentrations and increased the Cr(VI) reduction rates. Since iron did not increase (nor decreased) the reduction rates in cell suspensions, we conclude that Cr(VI) reduction in cultures was associated to cell multiplication and protection. Iron was therefore not involved in abiotic Cr(VI) reduction and there was no competition for a common reductase. In cell suspensions, the increase in Cr(VI) concentrations caused a linear increase in the reduction rates. The better performance of cell suspensions compared to cultures is likely due to the lower energy amount committed to cell proliferation and instead used for protection.

The presence of insoluble extracellular phosphate aggregates containing chromium (and also iron and calcium) was dependent of iron, and resulted in the efficient removal of chromium from solution by strain 5bvl1. This process was not responsible for Cr(VI) reduction since reduction without sedimentation was observed. Chromium immobilization in insoluble particles was a metabolic process inhibited by high Cr(VI) concentrations, and not a consequence of passive biosorption [47–50] or uptake [2,16]. Therefore, extracellular phosphate particle formation seems to be a cell response to Cr(VI) stress under beneficial Fe(III) concentrations, and not caused by membrane damage or disruption. In fact, the presence of iron in the culture medium also decreased the number of morphologically aberrant cells, which typically appear in Cr(VI) stressed cells [12,51].

Both strains tested, 5bvl1 and *O. tritici* type strain, were able to form extracellular phosphate aggregates in presence of both Fe(III) and Cr(VI) (or Ni(II)), but only strain 5bvl1 acted as an efficient and sustainable phosphate remover at high Cr(VI) concentrations. At high Cr(VI) concentrations (5 mM), the type strain appeared to rapidly release intracellular phosphate while this was not compensated by an uptake of free phosphate. This may be a response to toxicity, in consequence of its lack of chromate pump and of other protective proteins coded by the Tn*OtChr* transposon [12,15]. In strain 5bvl1, the final amount of phosphate removed from the medium corresponded to the phosphate quantity found in extracellular aggregates, and the process seemed to consist in a fast phosphate uptake from the medium and a progressive release as insoluble extracellular aggregates. Concerning this, Ni(II) had an effect comparable to Cr(VI), unlike paraquat, which leads to the conclusion that generated reactive oxygen species alone are not sufficient for extracellular aggregates production. Interestingly, a previous work [15] showed that paraquat also failed to induce Tn*OtChr* operon transcription.

Bacterial intracellular polyphosphate granules have been associated to several functions: Pi and cations reservoir, metal chelation, resistance to environmental stress, bacterial

transformation, capsule formation, virulence, quorum sensing, adaptation to nutritional stringencies, and survival in stationary phase of growth [16,52,53]. Pavlov et al. [54] also demonstrated the polyphosphate ability to form a non-proteinaceous transmembrane cation-selective channel. In the presence of Fe(III) and Cr(VI), intracellular phosphorus-rich granules were in fact detected in uncompromised cells of strain 5bvl1, but Cr was never detected in those structures, and rather found in extracellular aggregates. Cells cultured under those experimental conditions formed cellular aggregates strongly reactive to the Neisser stain, while cells not exposed to these metals were planktonic and Neisser-negative, failing to produce extracellular granules. This correlates with the observation of Rashid et al. [52], which linked polyphosphate to biofilm formation in *P. aeruginosa*.

Recent reports have linked phosphatase activity to metal bioprecipitation as phosphate complexes [41]. Although we cannot discard this activity for phosphate (re)acquisition, our results instead demonstrate a connection between PPK activity and chromium bioprecipitation. Exposure to Cr(VI) and Fe(III) increased the production of polyphosphate from ATP, indicating the presence of more active PPK than in the absence of metal ions [27,55]. Therefore, the PPK activity increase, in strain 5bvl1, can be correlated to the phosphate uptake and the formation of phosphate-rich extracellular aggregates. This is in agreement with the upregulation of storage proteins observed by Chourey et al. [44,45] in *S. oneidensis* MR-1, when subjected to Cr(VI).

The presence of polyphosphate in the extracellular aggregates was confirmed by ^{31}P NMR and FT-IR, which, together with EDS, defined their chemical composition and structure. ^{31}P NMR showed the presence of phosphonates, orthophosphate, polyphosphate, and possibly some pyrophosphate [19,28]. Since ^{31}P NMR essentially detects solubilized phosphate compounds, only uncomplexed Pi and polyphosphate (short chains) were possible to detect. The presence of phosphonates, together with polyphosphate, has been related in sea sediments to microbiological activity [19]. FT-IR revealed the presence of an intense signal typical of EPS C–O vibrations, which may be the consequence of biofilm formation [32]. The most important FT-IR signals present support the presence of both linear polyphosphate, possibly some pyrophosphate, and inorganic phosphate coordinated to Cr(III). Interestingly, both the sample of extracellular aggregates and the polyphosphate–Cr(III) control presented the same green color.

5. Conclusion

The most innovative aspect of this paper is the demonstration of the production by strain 5bvl1 of extracellular polyphosphate which participate in Cr(III) hydroxides chelation that result from bacterial Cr(VI) reduction, and its dependence of iron under Cr(VI) stress. In *O. tritici* strain 5bvl1, with exception of the *chr* genes responsible for Cr(VI) resistance, all the genes involved in the processes mentioned above are still unknown.

This work brings new information concerning the chromium toxicity protection mechanisms of *O. tritici* strain 5bvl1 in addition to the already described ChrA Cr(VI) pump and SOD related enzymes. According to the results obtained in this work, future investigation on the processes and genes involved in Cr(VI) removal will prove useful for the use of this strain in bioremediation.

Acknowledgements

This research was founded by FCT, Portugal, under PTDC/MAR/109057/2008 project. R. Francisco was supported by PhD grants from FCT. Professor A.L. Cunha, Institute of Biomedical Sciences Abel Salazar, Porto, Portugal, helped in sample thin-sectioning for SEM. SEM-EDS analysis was performed at CEMUP, Porto, Portugal.

References

[1] World Health Association, Guidelines for drinking-water quality – Chromium, in: World Health Association (Ed.), Guidelines for Drinking-Water Quality (vol. 1, Recommendations), World Health Association, Geneva, Switzerland, 1993, pp. 45–46.
[2] T.C. Hazen, H.H. Tabak, Developments in bioremediation of soils and sediments polluted with metals and radionuclides: 2. Field research on bioremediation of metals and radionuclides, Rev. Environ. Sci. Biotechnol. 4 (2005) 157–183.
[3] R. Elangovan, S. Abhipsa, B. Rohit, P. Ligy, K. Chandraraj, Reduction of Cr(VI) by a *Bacillus* sp., Biotechnol. Lett. 28 (2006) 247–252.
[4] F.A.O. Camargo, B.C. Okeke, F.M. Bento, W.T. Frankenberger, In vitro reduction of hexavalent chromium by a cell-free extract of *Bacillus* sp. ES 29 stimulated by Cu^{2+}, Appl. Microbiol. Biotechnol. 62 (2003) 569–573.
[5] B. Chardin, M.-T. Giudici-Orticoni, G. De Luca, B. Guigliarelli, M. Bruschi, Hydrogenases in sulfate-reducing bacteria function as chromium reductase, Appl. Microbiol. Biotechnol. 63 (2003) 315–321.
[6] T.L. Daulton, B.J. Little, K. Lowe, J. Jones-Meehan, In-situ environmental cell – transmission electron microscopy study of microbial reduction of chromium(VI) using electron energy loss spectroscopy, Microsc. Microanal. 7 (2001) 470–485.
[7] J.K. Fredrickson, H.M. Kostandarithes, S.W. Li, A.E. Plymale, M.J. Daly, Reduction of Fe(III), Cr(VI) U(VI), and Tc(VII) by *Deinococcus radiodurans* R1, Appl. Environ. Microbiol. 66 (2000) 2006–2011.
[8] C. Cervantes, J. Campos-Garcia, Reduction and efflux of chromate by bacteria, in: D.H. Nies, S. Silver (Eds.), Molecular Microbiology of Heavy Metals, Microbiol. Monogr. vol. 6, Springer-Verlag Berlin Heidelberg, 2007, pp. 407–419.
[9] M. Faisal, S. Hasnain, Microbial conversion of Cr (VI) in to Cr (III) in industrial effluent, Afr. J. Biotechnol. 3 (2004) 610–617.
[10] S. Sultan, S. Hasnain, Reduction of toxic hexavalent chromium by *Ochrobactrum intermedium* strain SDCr-5 stimulated by heavy metals, Bioresour. Technol. 98 (2007) 340–344.
[11] R. Branco, M.C. Alpoim, P.V. Morais, *Ochrobactrum tritici* strain 5bvl1 – characterization of a Cr(VI)-resistant and Cr(VI)-reducing strain, Can. J. Microbiol. 50 (2004) 697–703.
[12] R. Francisco, A. Moreno, P.V. Morais, Different physiological responses to chromate and dichromate in the chromium resistant and reducing strain *Ochrobactrum tritici* 5bvl1, Biometals 23 (2010) 713–725.
[13] N. Peitzsch, G. Eberz, D.H. Nies, *Alcaligenes eutrophus* as a bacterial chromate sensor, Appl. Environ. Microbiol. 64 (1998) 453–458.
[14] D.H. Nies, G. Rehbein, T. Hoffmann, C. Baumann, C. Grosse, Paralogs of genes encoding metal resistance proteins in *Cupriavidus metallidurans* strain CH34, Mol. Microbiol. Biotechnol. 11 (2006) 82–93.
[15] R. Branco, A.P. Chung, T. Johnston, V. Gurel, P.V. Morais, A. Zhitkovich, The chromate-inducible chrBACF operon from the transposable element Tn*OtChr* confers resistance to chromium(VI) and superoxide, J. Bacteriol. 190 (2008) 6996–7003.
[16] Y. Suzuki, J.F. Banfield, Resistance to, and accumulation of, uranium by bacteria from a uranium-contaminated site, Geomicrobiol. J. 21 (2004) 113–121.
[17] Y.V. Nancharaiah, C. Dodge, V.P. Venugopalan, S.V. Narasimhan, A.J. Francis, Immobilization of Cr(VI) and its reduction to Cr(III) phosphate by granular biofilms comprising a mixture of microbes, Appl. Environ. Microbiol. 76 (2010) 2433–2438.
[18] M. Ying, M. Rajkumar, H. Freitas, Improvement of plant growth and nickel uptake by nickel resistant-plant-growth promoting bacteria, J. Hazard. Mater. 166 (2009) 1154–1161.
[19] P. Sannigrahi, E. Ingall, Polyphosphates as a source of enhanced P fluxes in marine sediments overlain by anoxic waters: evidence from ^{31}P NMR, Geochem. Trans. 6 (2005) 52.
[20] R. Francisco, M.C. Alpoim, P.V. Morais, Diversity of chromium-resistant and -reducing bacteria in a chromium-contaminated activated sludge, J. Appl. Microbiol. 92 (2002) 837–843.
[21] R. Branco, A.P. Chung, P.V. Morais, Sequencing and expression of two arsenic resistance operons with different functions in the highly arsenic-resistant strain *Ochrobactrum tritici* SCII24T, BMC Microbiol. 8 (2008) 95.
[22] APHA, Metals, part 3000, in: L.S. Clesceri, A.E. Greenberg, A.D. Eaton (Eds.), Standard Methods for the Determination of Water and Wastewater, 20th ed., American Public Health Association, Washington, DC, 1998, pp. 65–68.
[23] B.L. Clark, Characterization of a catechol-type siderophore and the detection of a possible outer membrane receptor protein from *Rhizobium leguminosarum* strain IARI 312, Dissertation, Department of Health Sciences, East Tennessee State University, Johnson City, TN, 2004.
[24] J.D. Martin, Y. Ito, V.V. Homann, M.G. Havgood, A. Butler, Structure and membrane affinity of new amphiphilic siderophores produced by *Ochrobactrum* sp. SP18, J. Biol. Inorg. Chem. 11 (2006) 633–641.
[25] B.N. Ames, Assay of inorganic phosphate, total phosphate and phosphatases, Methods Enzymol. 8 (1966) 115–118.
[26] H.E. Morton, A. Francisco, The staining of the metachromatic granules in *Corynebacterium diphtheriae*, Biotech. Histochem. 17 (1942) 27–29.
[27] A. Mullan, J.P. Quinn, J.W. McGrath, A nonradioactive method for the assay of polyphosphate kinase activity and its application in the study of polyphosphate metabolism in *Burkholderia cepacia*, Anal. Biochem. 308 (2002) 294–299.

[28] E.C.O. Lima, J.M.M. Neto, F.Y. Fujiwara, F. Galembeck, Aluminum polyphosphate thermoreversible gels: a study by ^{31}P and ^{27}Al NMR spectroscopy, J. Colloid Interface Sci. 176 (1995) 388–396.
[29] Y.-L. Bai, H.-B. Xua, Y. Zhanga, Z.-H. Li, Reductive conversion of hexavalent chromium in the preparation of ultra-fine chromia powder, J. Phys. Chem. Solids 67 (2006) 2589–2595.
[30] Z. He, C.W. Honeycutt, T. Ohno, J.F. Hunt, B.J. Cade-Menun, Phosphorus features in FT-IR spectra of natural organic matter, Chin. J. Geochem. 25 (2006) 259.
[31] X.K. Zhang, E.G. Lewars, R.E. March, J.M. Pads, Vibrational spectrum of the acetone–water complex: a matrix isolation FTIR and theoretical study, J. Phys. Chem. 97 (1993) 4320–4325.
[32] M. Sekkal, C. Declerck, J.-P. Huvenne, P. Legrand, B. Sombret, M.-C. Verdus, Direct structural identification of polysaccharides from red algae by FTIR microspectrometry: II. Identification of the constituents of *Gracilaria verrucosa*, Mikrochim. Acta 112 (1993) 11–18.
[33] B.H. Stuart, Infrared Spectroscopy: Fundamentals and Applications Analytical Techniques in the Sciences (AnTs), John Wiley & Sons, 2004, ebook, ISBN: 0470854286, pp. 84–85.
[34] N.M. Bobkova, N.I. Zayants, M.P. Glasova, IR spectra of calcium phosphate–silicate glasses as the basis of biopyrocerams, J. Appl. Spectrosc. 61 (1994) 637–639.
[35] M.M.M. de Azevedo, M.-I.M.S. Bueno, C.U. Davanzo, F. Galembeck, Coexistence of liquid phases in the sodium polyphosphate–chromium nitrate–water system, J. Colloid Interface Sci. 248 (2002) 185–193.
[36] C. Ananthamohan, C.A. Hogarth, C.R. Theocharis, D. Yeates, Investigation of infrared absorption spectra of copper phosphate glasses containing some rare earth oxides, J. Mater. Sci. 25 (1990) 3956–3959.
[37] H. Fuks, S.M. Kaczmarek, M. Bosacka, EPR and IR investigations of some chromium (III) phosphate (V) compounds, Rev. Adv. Mater. Sci. 23 (2010) 57–63.
[38] M. Klähn, G. Mathias, C. Kötting, M. Nonella, J. Schlitter, K. Gerwert, P. Tavan, IR spectra of phosphate ions in aqueous solution: predictions of a DFT/MM approach compared with observations, J. Phys. Chem. A 108 (2004) 6186–6194.
[39] K. Senthil, R. Sarojini, Curcumin–DNA interaction studied by Fourier Transform Infrared spectroscopy, in: The Free Library, http://www.thefreelibrary.com/Curcumin-DNA interaction studied by Fourier Transform Infrared..-a0215925286 [cited 1 September 2009].
[40] A. Barth, F. von Germar, W. Kreutz, W. Mäntele, Time-resolved infrared spectroscopy of the Ca21-ATPase, J. Biol. Chem. 271 (1996) 30637–30646.
[41] R.J. Martinez, M.J. Beazley, M. Taillefert, A.K. Arakaki, J. Skolnick, P.A. Sobecky, Aerobic uranium (VI) bioprecipitation by metal-resistant bacteria isolated from radionuclide and metal-contaminated subsurface soils, Environ. Microbiol. 9 (2007) 3122–3133.
[42] L. Fude, B. Harris, M.M. Urrutia, T.J. Beveridge, Reduction of Cr(VI) by a consortium of sulfate-reducing bacteria (SRB-III), Appl. Environ. Microbiol. 60 (1994) 1525–1531.
[43] T. Nagata, M. Kiyono, H. Pan-Hou, Engineering expression of bacterial polyphosphate kinase in tobacco for mercury remediation, Appl. Microbiol. Biotechnol. 72 (2006) 777–782.
[44] K. Chourey, W. Wei, X.-F. Wan, D.K. Thompson, Transcriptome analysis reveals response regulator SO2426-mediated gene expression in *Shewanella oneidensis* MR-1 under chromate challenge, BMC Genomics 9 (2008) 395.
[45] K. Chourey, M.R. Thompson, J. Morrell-Falvey, N.C. VerBerkmoes, S.D. Brown, M. Shah, J. Zhou, M. Doktycz, R.L. Hettich, D.K. Thompson, Global molecular and morphological effects of 24-hour chromium(VI) exposure on *Shewanella oneidensis* MR-1, Appl. Environ. Microbiol. 72 (2006) 6331–6344.
[46] M.I. Ramirez-Diaz, C. Diaz-Perez, E. Vargas, H. Riveros-Rosas, J. Campos-Garcia, C. Cervantes, Mechanisms of bacterial resistance to chromium compounds, Biometals 21 (2008) 321–332.
[47] S.-Y. Kanga, J.-U. Lee, K.-W. Kim, Biosorption of Cr(III) and Cr(VI) onto the cell surface of *Pseudomonas aeruginosa*, Biochem. Eng. J. 36 (2007) 54–58.
[48] M. Nedelkova, M.L. Merroun, A. Rossberg, C. Hennig, S. Selenska-Pobell, Microbacterium isolates from the vicinity of a radioactive waste depository and their interactions with uranium, FEMS Microbiol. Ecol. 59 (2007) 694–705.
[49] M.L. Merroun, J. Raff, A. Rossberg, C. Hennig, T. Reich, S. Selenska-Pobell, Complexation of uranium by cells and S-layer sheets of *Bacillus sphaericus* JG-A12, Appl. Environ. Microbiol. 71 (2005) 5532–5543.
[50] J. McLean, T.J. Beveridge, Chromate reduction by Pseudomonad isolated from a site contaminated with chromated copper arsenate, Appl. Environ. Microbiol. 67 (2001) 1076–1084.
[51] B. Li, D. Pan, J. Zheng, Y. Cheng, X. Ma, F. Huang, Z. Lin, Microscopic investigations of the Cr(VI) uptake mechanism of living *Ochrobactrum anthropi*, Langmuir 24 (2008) 9630–9635.
[52] M.H. Rashid, K. Rumbaugh, L. Passador, D.G. Davies, A.N. Hamood, B.H. Iglewski, A. Kornberg, Polyphosphate kinase is essential for biofilm development, quorum sensing, and virulence of *Pseudomonas aeruginosa*, PNAS 97 (2000) 9636–9641.
[53] A. Kornberg, N.N. Rao, D. Ault-Riché, Inorganic polyphosphate: a molecule of many functions, Annu. Rev. Biochem. 68 (1999) 89–125.
[54] E. Pavlov, C. Grimbly, C.T.M. Diao, R.J. French, A high-conductance mode of a poly-3-hydroxybutyrate/calcium/polyphosphate channel isolated from competent *Escherichia coli* cells, FEBS Lett. 579 (2005) 5187–5192.
[55] R. Ohtomo, Y. Sekiguchi, T. Mimura, M. Saito, T. Ezawa, Quantification of polyphosphate: different sensitivities to short-chain polyphosphate using enzymatic and colorimetric methods as revealed by ion chromatography, Anal. Biochem. 328 (2004) 139–146.